

GA-A26114

**COMPARISON OF EDGE PLASMA PERTURBATIONS  
DURING ELM CONTROL USING ONE VS  
TWO TOROIDAL ROWS OF RMP COILS  
IN ITER SIMILAR SHAPED PLASMAS ON DIII-D**

by

**M.E. FENSTERMACHER, T.E. EVANS, T.H. OSBORNE, M.J. SCHAFFER,  
J.S. deGRASSIE, P. GOHIL, R.J. GROEBNER, R.A. MOYER,  
and the DIII-D TEAM**

**JANUARY 2009**



## **DISCLAIMER**

This report was prepared as an account of work sponsored by an agency of the United States Government. Neither the United States Government nor any agency thereof, nor any of their employees, makes any warranty, express or implied, or assumes any legal liability or responsibility for the accuracy, completeness, or usefulness of any information, apparatus, product, or process disclosed, or represents that its use would not infringe privately owned rights. Reference herein to any specific commercial product, process, or service by trade name, trademark, manufacturer, or otherwise, does not necessarily constitute or imply its endorsement, recommendation, or favoring by the United States Government or any agency thereof. The views and opinions of authors expressed herein do not necessarily state or reflect those of the United States Government or any agency thereof.

# COMPARISON OF EDGE PLASMA PERTURBATIONS DURING ELM CONTROL USING ONE VS TWO TOROIDAL ROWS OF RMP COILS IN ITER SIMILAR SHAPED PLASMAS ON DIII-D

by

M.E. FENSTERMACHER,\* T.E. EVANS, T.H. OSBORNE, M.J. SCHAFFER,  
J.S. deGRASSIE, P. GOHIL, R.J. GROEBNER, R.A. MOYER,<sup>†</sup>  
and the DIII-D TEAM

This is a preprint of a paper to be presented at the Eighteenth International Conference on Plasma Surface Interactions, May 26-30, 2008, in Toledo, Spain, and to be published in the *J. Nucl. Mater.*

\*Lawrence Livermore National Laboratory, Livermore, California.

<sup>†</sup>University of California-San Diego, La Jolla, California.

Work supported by  
the U.S. Department of Energy  
under DE-AC52-07NA27344, DE-FC02-04ER54698,  
and DE-FG02-07ER54917

GENERAL ATOMICS ATOMICS PROJECT 30200  
JANUARY 2009

## ABSTRACT

Large Type-I edge localized modes (ELMs) were suppressed by  $n = 3$  resonant magnetic perturbations (RMPs) from a set of internal coils in plasmas with an ITER similar shape at the ITER pedestal collisionality,  $\nu_e^* \sim 0.1$  and low edge safety factor ( $q_{95} \approx 3.6$ ), with either a single toroidal row of the internal RMP coils or two poloidally separated rows of coils. ELM suppression with a single row of internal coils was achieved at approximately the same  $q_{95}$  surface-averaged perturbation field as with two rows of coils, but required higher current per coil. Maintaining complete suppression of ELMs using  $n = 3$  RMPs from a single toroidal row of internal coils was less robust to variations in input neutral beam injection torque than previous ELM suppression cases using both rows of internal coils. With either configuration of RMP coils, maximum ELM size is correlated with the width of the edge region having good overlap of the magnetic islands from vacuum field calculations.

## I. INTRODUCTION

In high confinement (H-mode) tokamak plasmas, control of edge localized mode (ELM) instabilities is a critical issue for the operation of future large tokamaks including ITER [1] due to predictions of unacceptably high erosion of material surfaces by the heat and particle fluxes during these transient events. Various techniques to reduce ELM size or eliminate ELMs altogether are under investigation ([2] and references therein). Previous experiments in DIII-D have shown that ELMs can be suppressed in H-mode plasmas over a range of conditions (density, collisionality, input power, safety factor etc.) by applying  $n = 3$  resonant magnetic perturbations (RMPs) ([2] and references therein) [3-8] using two toroidal rows of internal, small aperture magnetic coils poloidally separated above and below the outer equatorial midplane. ELM mitigation has been obtained using  $n = 1$  and  $n = 2$  fields from a set of large aperture, midplane coils on JET [9,10], but ELM suppression has not been obtained on JET or in DIII-D experiments [11] even with  $n = 3$  fields from large aperture midplane coils. In a recent set of experiments described below, ELM suppression was achieved with  $n = 3$  RMPs using only one of the internal, toroidal, off-midplane rows of coils and then compared with similarly prepared ELM suppression discharges using both I-coil rows.

## II. EXPERIMENTAL RESULTS

The plasmas from the experiments reported in this paper had an ITER similar shape (ISS) and pedestal electron collisionality close to the value expected in ITER,  $\nu_e^* \sim 0.1$ . The plasma configuration and the geometry of the internal, off-midplane (I-coil) and external, on-midplane (C-coil) magnetic perturbation coils are shown in Fig. 1. These ISS plasmas had: plasma current  $I_p = 1.55$  MA, toroidal field  $B_T = 1.93$  T, lower triangularity  $\delta_{\text{lower}} = 0.67\text{--}0.70$ , upper triangularity  $\delta_{\text{upper}} = 0.36$ , elongation  $\kappa = 1.82$ , giving safety factor at 95% poloidal flux,  $q_{95} = 3.47\text{--}3.62$ . Injected neutral beam power was  $P_{\text{inj}} = 7.1\text{--}9.5$  MW, giving normalized beta  $\beta_N = \beta/(I_p/aB_T) = 1.7\text{--}2.4$ , where  $a$  is the minor radius of the plasma and  $\beta$  is the ratio of plasma pressure to magnetic field pressure.

Suppression of Type-I ELMs was achieved using a single I-coil row but more current per coil was required than for suppression with two rows of internal coils [11]. ELM suppression was obtained with 4.5 kAt per coil when using only the upper I-coil row [giving a surface-averaged  $n = 3$  resonant radial vacuum field in the  $m/n = 11/3$  component  $\delta b_r^{11/3} = 4.0$  G at  $\Psi_N = 0.95$ ] and at 4.8 kAt with only the lower I-coil row [ $\delta b_r^{11/3} = 4.2$  G at  $\Psi_N = 0.95$ ]. For comparison, ELM suppression was obtained in a similarly prepared discharge on the same experimental day using both the upper and the lower I-coil rows (2.9 and 2.5 kAt respectively giving  $\delta b_r^{11/3} = 4.6$  G at  $\Psi_N = 0.95$ ). A scan of the current in the single upper I-coil row showed the minimum current required to suppress ELMs was between 4.0 and 4.5 kAt (i.e. ( $\delta b_r^{11/3} = 3.5\text{--}4.0$  G at  $\Psi_N = 0.95$ ), i.e. at least 50% higher current per coil was required to achieve similar perturbation strength at the pedestal than when both I-coil rows are used, consistent with the difference in coil geometry. Comparing the poloidal mode spectra [12] for the case with the upper I-coil versus the case with both I-coils [11] showed similar  $\delta b_r^{11/3}$  at  $\Psi_N = 0.95$ , but significantly different resonant and non-resonant components elsewhere.

Initial tests showed that ELM suppression using a single row of  $n = 3$  RMP coils may be somewhat less robust to reductions in co- $I_p$  injected neutral beam torque than suppression using both rows of I-coils. Figure 2 shows a direct comparison of identically prepared successive discharges with the upper I-coil row at 4.5 kAt vs. both I-coil rows at 3.5 kAt in which the co- $I_p$  injected NB torque was reduced in steps during the RMP ELM suppressed phase. Note that for the I-coil currents used, the resonant perturbation at the pedestal in the two row case,  $\delta b_r^{11/3} = 5.8$  G, is higher than in the case with the upper row alone,  $\delta b_r^{11/3} = 4.2$  G. In the case with just the upper I-coil, both the pedestal toroidal rotation and beta

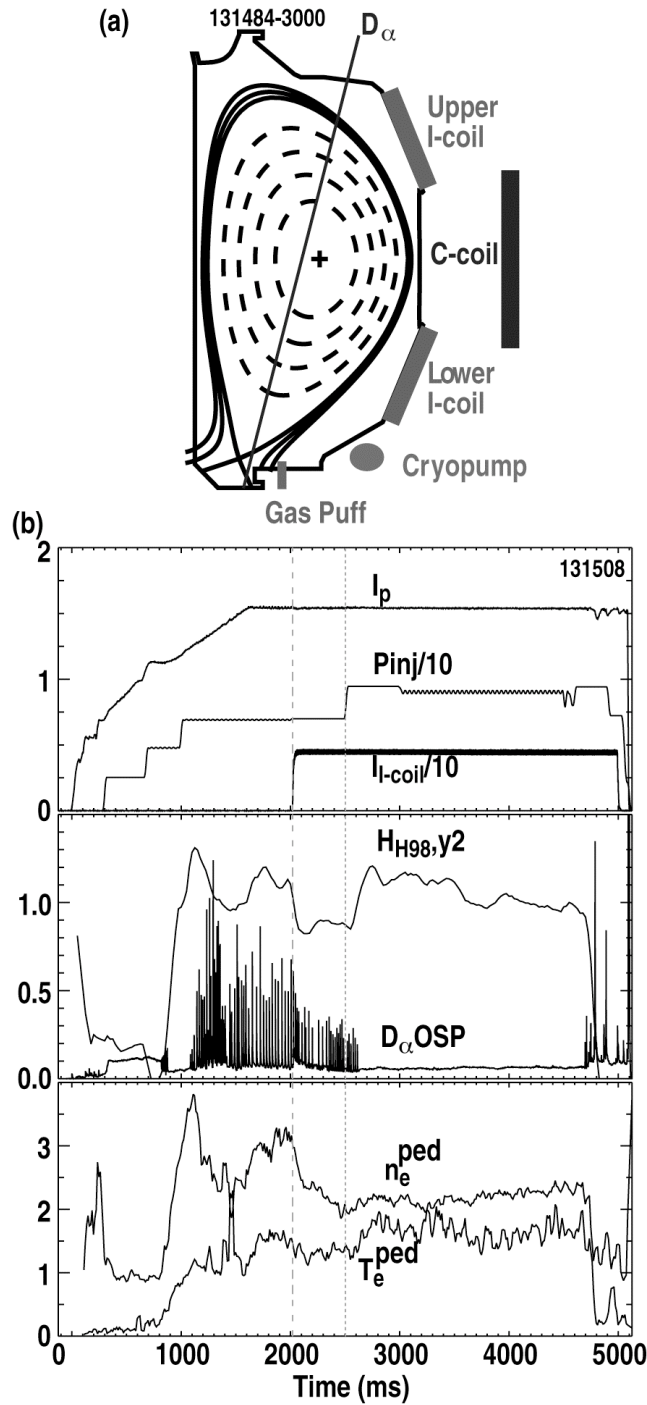


Fig. 1. Overview of operational parameters for discharges in this study including (a) plasma and coil geometry of the high triangularity ISS showing the optimal position of the outer strike point for pumping, the location of the  $D_\alpha$  line integrated measurement, and the locations of the I- and C-coils, and (b) temporal evolution of basic discharge parameters including plasma current [ $I_p$  (MA)], injected neutral beam power [ $P_{inj}$  (10 MW)], I-coil current [ $I_{I-coil}$  (10 kAt)]; confinement enhancement factor  $H(98,y2)$  and divertor outer strikepoint  $D_\alpha$  intensity ( $1 \times 10^{20}$  phot/ $m^2/s/str$ ); pedestal electron density [ $n_e^{ped}$  ( $10^{19} m^{-3}$ )] and temperature [ $T_e^{ped}$  (keV)]. I-coil on and power increase times marked by vertical dashed and dotted lines, respectively.

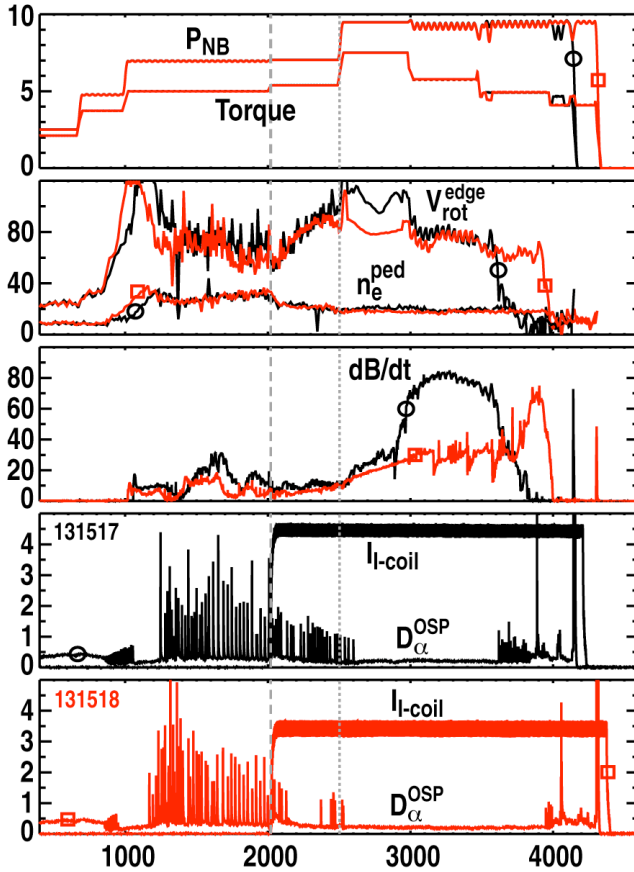


Fig. 2. Comparison of parameters from plasmas using one vs two I-coil rows in which input NBI torque is reduced in steps during the RMP phase for upper I-coil alone at 4.5 kAt and low density (black-circle), and both I-coils at 3.5 kAt and low pedestal density (red-square), including (a) injected co-current neutral beam torque (N-m) and injected NB power (MW), (b) pedestal density ( $10^{18} \text{ m}^{-3}$ ) and toroidal rotation in the edge pedestal (km/s), (c) amplitude of core MHD activity (T/s) and (d-e) outer divertor  $D_\alpha$  intensity ( $2.5 \times 10^{19} \text{ phot/m}^2/\text{s/str}$ ) and I-coil current (kAt). I-coil on and power increase times marked by vertical dashed and dotted lines respectively.

decrease, and transient activity on the divertor  $D_\alpha$  signal returns about 100 ms after the reduction of injected torque to 4.9 N-m. In the case with both I-coil rows, ELM suppression is retained for over 450 ms at 4.9 N-m torque. Although there are differences in the core MHD activity [Fig. 2(c)] between the two discharges, the edge rotation [Fig. 2(b)] is very similar prior to the step down in torque from 5.8 N-m to 4.9 N-m. As reported previously [8], the return of transient activity on divertor  $D_\alpha$  signals at reduced co- $I_p$  NB torque input is correlated with the reduction of the edge toroidal rotation below 40 km/s in DIII-D [Fig. 2(b)]. This initial experiment suggests that the edge rotation is more sensitive to reduced torque input during the ELM suppressed phase in the case with a single I-coil row compared to the case with both I-coil rows, even though the resonant perturbation strength at the pedestal is higher in the two row case. This suggests a need for further experiments to obtain detailed physics understanding of the contribution of the differences in resonant perturbation deeper into the core plasma and especially non-resonant components of the RMP mode spectra toward this sensitivity (see Ref. [11]).

### III. DISCUSSION OF THEORY — EXPERIMENT COMPARISON

In previous work [2], the width of the edge region having good overlap of the magnetic islands from the RMP in vacuum field calculations was a good ordering parameter for the maximum ELM size during the RMP. From the recent experiments comparing ELM control with a single toroidal row of I-coils versus both rows of I-coils, a database was formed of ELM size versus the width of the edge region having good overlap of magnetic islands from vacuum field calculations. The procedure for populating the database is described in detail in Ref. [2]; only a brief outline of the steps is given here. The discharges used in the database for this paper are shown in Fig. 3. In each case, analytic fits (hyperbolic tangent or spline) of the full set of electron and ion density and temperature radial profiles for a given timeslice were used in equilibrium reconstructions to generate flux surfaces and safety factor profiles that take into account the edge bootstrap current peak in H-mode (“kinetic” EFITs). Mode spectral analysis [12] of the vacuum RMP magnetic perturbation fields was done using these “kinetic” EFITs to determine the spatial location and calculated width of the magnetic islands in the edge plasma due to the RMP. For each pair of magnetic islands the Chirikov parameter (average island width divided by island spacing) was calculated. Finally, the width of the region having good overlap of the islands (Chirikov parameter  $> 1.0$ ) was determined from a spline fit of the radial profile of the Chirikov parameter in the edge [11,12].

The maximum ELM size obtained in discharges with the RMP from a single row of I-coils follows the ordering with the width of the edge region having overlap of the magnetic islands from the RMP (Fig. 4), as was found previously in studies with RMP from both I-coils [2]. This is not completely unexpected since the discharges in the database from Ref. [2] and the discharges in the present study have the same ISS configuration, the same edge safety factor  $q_{95} = 3.6$ , similar beam power and  $n = 3$  RMP fields. Figure 4(b) shows many of the same qualitative features found in the database of discharges with two rows of RMP coils. There is a clear decrease in the maximum ELM size, down to a level below the sensitivity of the ELM detection diagnostic, when the effect of the RMP is sufficiently strong that the width of the overlap region measured in  $\Psi_N$  exceeds a threshold value ( $\Delta_{\text{chir}>1} = 0.132$  in this case). In addition, there is a reduction in the maximum ELM size over a range of overlap widths ( $0.12 < \Delta_{\text{chir}>1} < 0.132$ ) for timeslices shortly after application of the RMP, in which small high frequency ELMs were still obtained. Both of these features were found in the previous database using discharges with RMP from both I-coils.

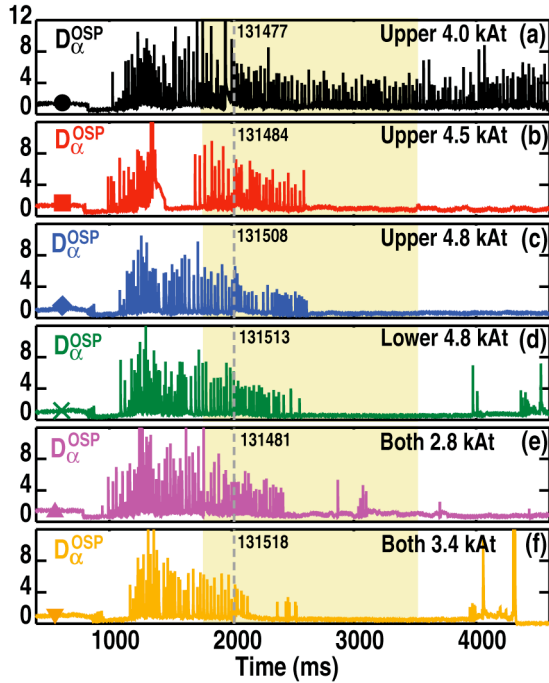


Fig. 3. Temporal evolution of outer divertor  $D_{\alpha}$  intensity ( $1 \times 10^{19}$  phot/m<sup>2</sup>/s/str) for the discharges in the database of ELM size vs island overlap region width using (a) the upper I-coil alone at 4.0 kAt and moderate pedestal density (black-circle), (b) the upper I-coil alone at 4.8 kAt and moderate pedestal density (red-square), (c) the upper I-coil alone at 4.8 kAt and low pedestal density (blue-diamond), (d) the lower I-coil alone at 4.8 kAt and low pedestal density (green-cross), (e) both I-coils simultaneously at 2.8 kAt and low pedestal density (magenta-triangle), and (f) both I-coils simultaneously at 3.4 kAt and low pedestal density (yellow-inverted triangle). RMP turn-on time is shown by the vertical dashed line. The range of times contributing to the database of Fig. 4 is shown by the shaded region.

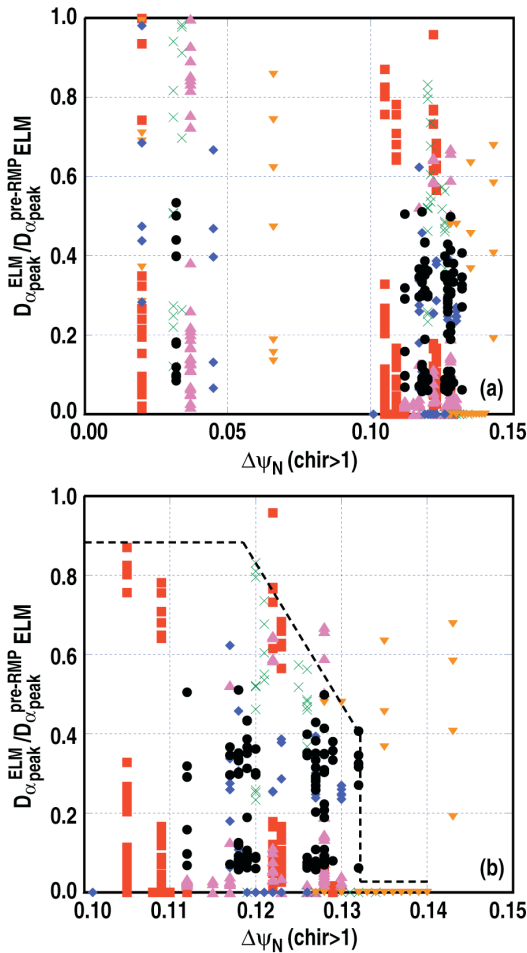


Fig. 4. Peak magnitude of ELM transient on outer strikepoint  $D_{\alpha}$  signal as a function of the width in normalized flux of the vacuum island overlap region with Chirikov parameter  $>1.0$  [ $\Delta\Psi_N(chir > 1)$ ] for multiple transients in the discharges from Fig. 3(a-f). (a) The value of ELM size plotted is normalized to the maximum size of the ELMs in the H-mode phase prior to application of the I-coil RMP field for each discharge, and (b) plot expanded for timeslices with the RMP coil on. Transients from a given discharge in Fig. 3 are marked with the same color and symbol used to identify the discharge in Fig. 3.

The similarity of the maximum ELM size ordering with width of the overlap region for the two databases supports a design guidance criterion of a minimum required overlap region width for ELM suppression, but differences between the results from the present database and those from the previous experiments [2] highlight limitations to the interpretation of this criterion. The threshold width for suppression in the present database is  $\Delta_{\text{chir}>1} = 0.132$ , lower than the value found in the previous experiments  $\Delta_{\text{chir}>1} = 0.165$ . In addition, there are a significant number of outliers in the ordering for both databases, i.e. ELMs for timeslices in which the overlap width is greater than the threshold. Finally, there are many timeslices, especially in the present database, for which no detectable ELMs are seen even though the overlap region width is less than the threshold. These observations clearly show that a design guidance criterion of a minimum required overlap region width from vacuum field calculations does not represent all of the important physics determining RMP ELM suppression. The contribution of many other factors must be taken into account for confident prediction of RMP ELM suppression in future devices, including the modification of the vacuum fields by the plasma response, the dependence of this modification on plasma rotation (screening) or plasma beta (amplification), enhanced transport across nested but non-axisymmetric surfaces, the contribution of wall conditions (pumping or source) to the effect of the RMP on the pedestal density profile, and the contribution of core MHD activity to the edge conditions. As an example, there are indications from an experiment with the upper I-coil alone and step changes in the injected neutral beam power (Ref. [11] Fig. 3), and also from the experiment in Fig. 2, that a threshold value of beta was required to achieve ELM suppression. For now, a design guidance criterion of a minimum required overlap region width serves only as a zeroth order guide to designs of RMP coil systems for ELM control in future tokamaks and should not be interpreted as describing the physics dominating ELM suppression by RMPs.

## IV. CONCLUSIONS

Suppression of ELMs using  $n = 3$  Resonant Magnetic Perturbations from internal coils in DIII-D was achieved in ITER similar shaped plasmas at the ITER pedestal collisionality,  $\nu_e^* \sim 0.1$  and low safety factor ( $q_{95} \approx 3.6$ ), with either a single toroidal row of the internal RMP coils or two poloidally separated rows of coils. The width of the region in the plasma edge with good overlap of the RMP magnetic islands from vacuum field calculations is an ordering parameter for the maximum ELM size during the RMP for either RMPs from one row or two poloidally separated rows of internal  $n = 3$  RMP coils, although outliers in the ordering point to important contributions from additional physics mechanisms. Initial experiments suggest that ELM suppression using a single off-midplane row of  $n = 3$  RMP coils is less robust to reductions in co- $I_p$  injected input torque than ELM suppression using two poloidally separated rows of  $n = 3$  RMP coils. Detailed physics understanding of the modification of the vacuum fields in the edge plasma by the plasma response, the effect of core MHD activity on the edge conditions, and the importance of material surface conditions on achieving the pedestal conditions necessary for ELM suppression is needed for confident prediction of RMP ELM suppression in future tokamak plasmas. Experiments are underway to obtain this physics understanding.

## REFERENCES

- [1] ITER Physics Basis Editors, Nucl. Fusion **39** (1999) 2137; ITER Physics Basis Editors, Nucl. Fusion **47** (2007) S1.
- [2] M.E. Fenstermacher, et al., Phys. Plasmas **15** (2008) 056122.
- [3] T.E. Evans, et al., Phys. Rev. Lett. **92** (2004) 235003.
- [4] T.E. Evans, et al., Nucl. Fusion **45** (2005) 595.
- [5] R.A. Moyer, et al., Phys. Plasmas **12** (2005) 056119.
- [6] K.H. Burrell, et al., Plasmas Phys. Control. Fusion **47** (2005) B37.
- [7] T.E. Evans, et al., Plasma Phys. **13** (2006) 056121.
- [8] T.E. Evans, et al., Nucl. Fusion **48** (2008) 024002.
- [9] Y. Liang, et al., Phys. Rev. Lett. **98** (2007 ) 265004
- [10] Y. Liang, et al., Plasma Phys. Control. Fusion **49** (2007) B581-589.
- [11] M.E. Fenstermacher, et al., Nucl. Fusion Lett. **48** (2008) 122001.
- [12] M.J. Schaffer, et al., Nucl. Fusion **48** (2008) 024004.

## **ACKNOWLEDGMENT**

This work was supported by the US Department of Energy under DE-AC52-07NA27344, DE-FC02-04ER54698 and DE-FG03-07ER54917.